

A TRIANGULAR PLATE BENDING ELEMENT FOR CONTACT PROBLEMS

OTTO J. SVEC and G. M. L. GLADWELL

Department of Civil Engineering, University of Waterloo, Waterloo, Ontario, Canada

Abstract—A refined triangular plate bending element is developed for the problem of a thin elastic plate resting on an elastic half-space. The behaviour of the elastic half-space is described in terms of displacements at ten points in each triangular region into which the surface in contact with the plate is divided. The plate finite element similarly has ten nodes. The requirements of continuity of displacement and slope between adjacent plate elements are met by using a seventh order polynomial with 33 degrees of freedom. The behaviour of this element is tested on various plate bending problems and found to be satisfactory. The element is then applied to the problems of square, triangular and circular plates resting on an elastic half-space and on a foundation of Winkler type, and some comments are made on the problem of finding an equivalent Winkler foundation for a given elastic half-space.

1. INTRODUCTION

THERE is no known exact solution for the problem of a finite plate resting on a semi-infinite elastic continuum, and the most promising numerical method seems to be the finite element method. Cheung and Zienkiewicz [1] and Cheung and Nag [2] have used this approach. Two of the important characteristics of their solutions are that they use rectangular plate bending elements and that they assume that the contact pressure is uniformly distributed around each nodal point. Their first assumption restricts their analysis to plates of rectangular form while the second leads to an unrealistic contact pressure distribution.

In order to lift the first restriction we have assumed that both the plate and the surface of the elastic half-space are divided into a number of triangular regions. To lift the second we have supposed that the contact pressure may be represented by a cubic polynomial on each of the triangular regions; such a polynomial will involve 10 coefficients.

The response of the surface of the elastic half-space to such a pressure can be determined from Boussinesq's equation

$$w(x, y) = d \int_A \int \frac{p(\xi, \eta) d\xi d\eta}{\sqrt{(x-\xi)^2 + (y-\eta)^2}}.$$

This equation expresses a continuous displacement $w(x, y)$ in terms of a continuous pressure $p(\xi, \eta)$. For use in a finite element analysis the equation must be discretized and inverted to give the 10 coefficients in the cubic expansion of p in terms of 10 displacement or slope quantities. The most convenient quantities would be those which are used in the usual triangular finite element analysis of a plate in bending, namely w , $\partial w/\partial x$, $\partial w/\partial y$ at the vertices and $\partial w/\partial n$ on one side [3].

Unfortunately, Svec and Gladwell [4] have shown that, even for a uniformly loaded triangular region on the surface of an elastic half-space the normal slope at a point on the

boundary and the slopes at a vertex all become infinite. This means that such slopes cannot be used and the half-space analysis must be phrased in terms of 10 proper displacements. In order to match the elastic half-space element we had to create a new plate bending element which had 10 nodal points and which included the displacements at these points among its generalized coordinates. This paper describes this element: it has 33 degrees of freedom and a deflection field represented by a polynomial of the seventh degree. The analysis is applied to the problem of a plate on a Winkler foundation and the results are compared to those for an elastic half-space which are derived in a companion paper by Svec and McNeice [5].

2. THE GENERALIZED DISPLACEMENT VECTOR

Ženišek [6] has discussed a large class of triangular finite elements. He has shown, in particular, that if the deflection function $w(x, y)$ is a seventh order polynomial it may be specified by means of the following quantities:

the six quantities $\partial^{i+j}w(P_k)/\partial x^i \partial y^j$, $i+j \leq 2$ at each of the three vertices; the three quantities $\partial^{i+j}w(P_0)/\partial x^i \partial y^j$, $i+j \leq 1$ at the centroid P_0 ; the displacements $w(Q_k^{(2)})$ at two points on each side; the slopes $\partial w(Q_s^{(3)})/\partial n$ at three points on each side.

The points at which the quantities are evaluated are shown in Fig. 1. Thus, in addition to the vertices, there are on each side two points at which the displacement is evaluated and three at which the slope is required, five points in all. The total number of nodes is 19. This can be reduced to 13 by making the $6Q_k^{(2)}$ points coincide with 6 of the $Q_s^{(3)}$ points. In order to reduce the total number of points to 10 one must inspect the deflection function more closely.

On any one side of the triangle the deflection function may be written as a polynomial of the seventh degree in the distance coordinate s . Its 8 coefficients may be determined uniquely by the known values of w , $\partial w/\partial s$, $\partial^2 w/\partial s^2$ at the 2 vertices, and w at the $2Q_k^{(2)}$ points. The normal slope $\partial w/\partial n$ will be a polynomial of the sixth degree on the side and will be determined by the known values of $\partial w/\partial n$, $\partial^2 w/\partial n \partial s$ at the 2 vertices and $\partial w/\partial n$ at the $3Q_s^{(3)}$ points, seven quantities in all. Both w and $\partial w/\partial n$ will be continuous across the boundary between two adjacent elements. To reduce the number of required nodes on each side by one, that is, to eliminate the need for the third $Q_s^{(3)}$ point on each side, we demand

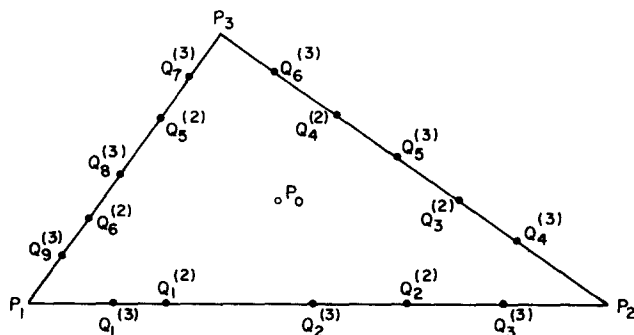


FIG. 1. The nodal points in Ženišek's model.

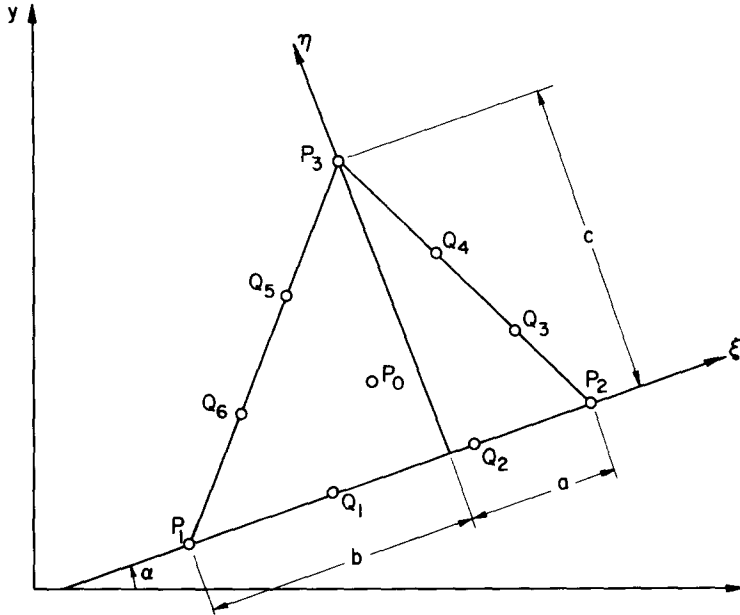


FIG. 2. The geometry of the chosen finite element.

that the normal slope $\partial w/\partial n$ shall be a polynomial of the fifth degree on each side. The Q points will be taken at the points of trisection of the sides, as shown in Fig. 2, and the polynomial is taken to be

$$w = a_1 + a_2\eta + a_3\xi + a_4\eta^2 + a_5\xi\eta + \dots, a_{36}\xi^7.$$

This may be written

$$w = \sum_{i=1}^{36} a_i \xi^{m_i} \eta^{n_i}, \tag{1}$$

where

$$i = k(k+1)/2 + l, \quad l = 1, 2, \dots, k+1, \quad k = 0, 1, \dots, 7,$$

$$m_i = l - 1,$$

$$n_i = k - l + 1.$$

The resulting conditions are then

$$a_{35} = 0 \tag{2}$$

$$7b^6ca_{29} + (5b^4c^3 - 2b^6c)a_{30} + (4b^3c^4 - 3b^5c^2)a_{31} + (3b^2c^5 - 4b^4c^3)a_{32} + (2bc^6 - 5b^3c^4)a_{33} + (c^7 - 6b^2c^5)a_{34} - 7bc^6a_{36} = 0, \tag{3}$$

$$7a^6ca_{29} + (5a^4c^3 - 2a^6c)a_{30} + (3a^5c^2 - 4a^3c^4)a_{31} + (3a^2c^5 - 4a^4c^3)a_{32} + (5a^3c^4 - 2ac^6)a_{33} + (c^7 - 6a^2c^5)a_{34} + 7ac^6a_{36} = 0. \tag{4}$$

The displacement and slope will still be continuous across the boundary between adjacent elements.

Each degree of freedom in the column vector of generalized displacements for the triangle may now be expressed in terms of the 36 coefficients of the deflection function. In matrix form the relation is

$$\begin{Bmatrix} w \\ w_{\xi} \\ w_{\eta} \\ w_{\xi\xi} \\ w_{\xi\eta} \\ w_{\eta\eta} \\ w \\ w_n \end{Bmatrix} = [B_1] \{a\}. \quad (5)$$

The column vector $\{w\}$ contains the values of $w, w_{\xi}, w_{\eta}, w_{\xi\xi}, w_{\xi\eta}, w_{\eta\eta}$ at each of the three vertices; w, w_n at each of the six side nodes; w, w_{ξ}, w_{η} at the centroid. The last three rows of equation (5) express the three conditions (2-4). By inverting $[B_1]$ and omitting the last three columns of $[B_1]^{-1}$ we get

$$\{a\} = [B_2] \{w\}, \quad (6)$$

where $[B_2]$ has dimensions 36×33 .

3. THE STIFFNESS MATRIX

This may be obtained by the standard procedure. In the classical theory of bending for a uniform thin isotropic plate the strain energy of an element is

$$U = \frac{1}{2} D \int_A \int [w_{\xi\xi}^2 + w_{\eta\eta}^2 + 2\nu w_{\xi\xi} w_{\eta\eta} + 2(1-\nu)w_{\xi\eta}^2] d\xi d\eta$$

where $D = Eh^3/[12(1-\nu^2)]$ is the flexural rigidity, ν is Poisson's ratio and E is Young's modulus. It is found that for the deflection function (1) the strain energy may be written as

$$U = \frac{1}{2} D a^T K a, \quad (7)$$

where

$$\begin{aligned} k_{ij} = & m_i(m_i-1)m_j(m_j-1)F(m_i+m_j-4, n_i+n_j) \\ & + n_i(n_i-1)n_j(n_j-1)F(m_i+m_j, n_i+n_j-4) \\ & + \{2(1-\nu)m_i n_i m_j n_j + \nu n_i(m_i-1)n_j(n_j-1) \\ & + \nu n_i(n_i-1)m_j(m_j-1)\}F(m_i+m_j-2, n_i+n_j-2), \end{aligned}$$

and

$$F(m, n) = c^{m+1} [a^{m+1} - (-b)^{m+1}] m! n! / (m+n+2)!.$$

Details of the procedure for integrating over the triangular element may be found in [7]. Equations (6) and (7) may now be combined to give

$$U = \frac{1}{2} D \{w\}^T [K_1] \{w\},$$

where

$$[K_1] = [B_2]^T [K] [B_2]$$

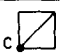


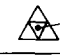


is the element stiffness matrix for the local coordinate system. Transformation to a global system may be performed in the standard manner.

4. ACCURACY OF THE ELEMENT

The finite element described above was tested on three plates: square, triangular and circular. The results are assembled in Table 1. A glance at the table will show that the element gives results which are slightly better than those obtained in [7] for the same mesh, and slightly worse than those obtained in [7] for a comparable number of degrees of freedom.

The results labelled 'exact' for the clamped square plate are the best results obtained in [7], using 119 degrees of freedom for $\frac{1}{8}$ of the plate.

TABLE 1. THE VERTICAL DISPLACEMENT AT THE CENTROID *c* OF SQUARE, TRIANGULAR AND CIRCULAR PLATES, FOR POISSON'S RATIO, $\nu = 0.3$.

MESH	DEGREES OF FREEDOM	SIMPLY SUPPORTED PLATE		DEGREES OF FREEDOM	CLAMPED PLATE	
		UNIFORM LOAD	POINT LOAD		UNIFORM LOAD	POINT LOAD
		$10^3 wD/qL^4$	$10^2 wD/PL^2$		$10^3 wD/qL^4$	$10^3 wD/PL^2$
	26	4.06228	1.157936	19	1.26609	5.59065
REF. 7	8	4.060937	1.149279	5	1.261295	5.534638
	52	4.062352	1.159527	45	1.26430	5.60691
	REF. 7	28	4.062347	1.1574224	21	1.2643177
EXACT		4.0623527	1.1600836		1.2653171	5.6090605
		$10^4 wD/qL^4$	$10^3 wD/PL^2$		$10^4 wD/qL^4$	$10^3 wD/PL^2$
	12	5.7870372	3.629886	6	1.652022	1.389904
REF. 7	3	3.472222	1.78195		—	—
	48	5.7871474	4.14425	33	1.676641	1.86304
	REF. 7	12	5.86276	3.92237		—
EXACT		5.787037	4.28479			
		$10^2 wD/qr^4$	$10^2 wD/Pr^2$		$10^2 wD/qr^4$	$10^2 wD/Pr^2$
	49	4.76549	4.073803	36	1.48088	1.93184
REF. 7	16	6.41040	—	8	1.6688	—
	57	6.45589	5.08874	52	2.08116	2.517824
	EXACT		6.37019	5.0501		1.5625

A calculation for one example, namely the simply-supported square plate under a uniformly distributed load gave the (dimensionless) strain energy values shown in Table 2. Table 1 shows that the results for vertical displacement obtained in Ref. [7] for 28 degrees of freedom were better than those obtained by using 26 degrees of freedom in the present method. Table 2 shows, on the other hand, that the results for strain energy were poorer than those obtained here.

TABLE 2. A COMPARISON OF DIMENSIONLESS STRAIN ENERGY VALUES FOR THE PRESENT METHOD AND THAT OF REFERENCE [7].

	Ref. 7		This work
28	8.5124403	26	8.5125433
63	8.5125406	52	8.5125513
Exact Solution			8.5125526

The results for the circular plate, at the bottom of the table, show that the extra side nodes, which allow a better satisfaction of the boundary conditions for polygonal plates, can be a disadvantage when used for circular plates. The first set of results, for the simply-supported circular plate, are poor compared with those of [7]. The reason for this is that the simply-supported boundary conditions have been applied to side nodes (which are on chords) and not just to nodes on the circular boundary as in [7]. The second set of results, distinguished by an asterisk, have been obtained by releasing the side nodes. This procedure improves the results for the simply-supported plate. For the clamped plate the satisfaction of boundary conditions at side nodes yields results which are good compared to those of [7] and much better than those obtained by releasing the side nodes.

5. PLATE ON WINKLER FOUNDATION

The foundation is characterized by

$$p(x, y) = kw(x, y), \quad (8)$$

where k is the foundation modulus. There are basically two ways of calculating the foundation stiffness matrix. The first (denoted by W1) is to assume that the pressure is uniformly distributed around each nodal point, as shown in Fig. 3. The stiffness matrix, denoted by $k[N_1]$ is a diagonal matrix. The coefficients of $[N_1]$ corresponding to corner points are 2δ to mid-side nodes 6δ , and the centroid 12δ , where $\delta = A/54$ and A is the element area. In the second approach (denoted by W2) it is assumed that the pressure can be represented by a cubic polynomial within each element. Equation (8) shows that this is equivalent to representing $w(x, y)$ by a cubic, so that

$$w(x, y) = \{L^T(x, y)\} \{A\}.$$

The coefficient vector $\{A\}$ may be expressed in terms of the nodal displacements so that

$$\{w\} = [T]\{A\}.$$

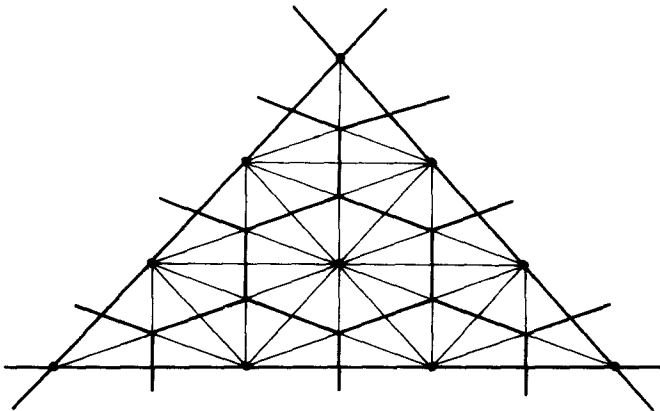


FIG. 3. The constant pressure regions for the first Winkler model.

The stiffness matrix may be obtained by equating the work done by the nodal forces to the work done by the continuous pressures. Thus

$$\begin{aligned}\{w\}^T\{F\} &= \int_A p(x, y)w(x, y) dA = k \int_A w^2(x, y) dA \\ &= k\{A\}^T[N]\{A\} = k\{w\}^T[T]^{-T}[N][T]^{-1}\{w\} \\ &= k\{w\}^T[N_2]\{w\}\end{aligned}$$

so that

$$\{F\} = k[N_2]\{w\}, \quad [N_2] = [T]^{-T}[N][T]^{-1}.$$

The equations may now be assembled by the usual finite element procedure. Because of equation (8) the assembly will yield C^0 continuity of $p(x, y)$ and of the displacement $w(x, y)$ of the foundation: the displacement of the plate will have C^1 continuity. Notice that $[N_2]$ is not diagonal so that nodal points within each element are bound together by some kind of cross springs. This means that this foundation model lies between a pure Winkler foundation and the elastic half-space.

6. EXAMPLES

The total system of equations for the plate resting on an elastic half-space were developed by Svec and McNeice [5] using the plate finite element described in this paper, and are

$$\{Q\} = D([K] + \alpha_1[S])\{w\} \quad (9)$$

where $\{Q\}$ is the vector of external loads, $[K]$ is the stiffness matrix of the plate, $[S]$ is the stiffness matrix of the elastic half-space and $\{w\}$ is a vector consisting of the nodal vertical displacements common to the plate and the foundation as well as the nodal plate slopes and curvatures. Furthermore,

$$\alpha_1 = \frac{1}{\alpha D} = \frac{E_0 \pi 12(1 - \nu^2)}{E h^3(1 - \nu_0^2)} = \frac{E_0}{E} \cdot c = \frac{1}{\gamma} c,$$

where E , ν and E_0 , ν_0 are the Young's modulus and Poisson's ratio of the plate and foundation, respectively, and h is the plate thickness. The stiffness of the plate relative to the half-space is a function of γ , ν , ν_0 and h and a proper parametric study would include variations in all these quantities, but particularly in γ and h . In this paper, we show the variation only with γ , while ν , ν_0 , h are kept constant. For the values of ν , ν_0 and h used in this paper, c has the value 4410.8. The total systems of equations for the plate on a Winkler foundation W1 or W2 are

$$\{Q\} = D([K] + \alpha_2[N_i])\{w\} \quad i = 1, 2, (\text{W1, W2}),$$

where

$$\alpha_2 = \frac{k}{D} = \frac{k 12(1 - \nu^2)}{E h^3} = \frac{k}{E} \frac{(1 - \nu_0^2)}{\pi} c = \frac{1}{\beta} c.$$

In order to compare results for a pure Winkler model with those for the elastic half-space, the resulting step function representing the contact pressure for the Winkler model is always drawn as a smooth curve. This should be kept in mind while evaluating the results obtained.

Displacements and pressures for a circular plate subject to a uniform load are shown in Fig. 4. For large $\gamma = (10,000)$ and $\beta (= 3000)$, i.e. a comparatively rigid plate, the displacements for all three cases, and the contact pressures for both Winkler models are almost uniform. Only the contact pressure for the elastic half-space varies substantially across the radius, with high concentration at the edges. As the plate becomes weaker (i.e. γ and β decrease) the discrepancies between the three models become smaller.

The calculated curves of contact pressure denoted by $\gamma = 1$ in Fig. 4 can be seen to be unrealistic. If $\gamma = 1$ the plate is relatively weak so that loads applied to it will pass right through as if it were not there at all. Thus, the contact pressure in this case should be the applied uniform load: in other words, the curve of P should be the straight line $P = 1$. The reason for the breakdown in the theory can be seen by inspecting equation (9). The loads $\{Q\}$ on the right hand side are the nodal loads which are equivalent to the uniform load, in the sense of virtual work calculated on the basis of the plate displacements. These loads are not equivalent to the uniform load for displacements of the half-space. When the half-space is much less stiff than the plate, so that the term $D \times_1[S]$, which gives the additional stiffness supplied by the half-space, is small, the fact that $\{Q\}$ is calculated using plate displacements, makes very little difference. But when $D \times_1[S]$ is the dominant term the discrepancy becomes noticeable.

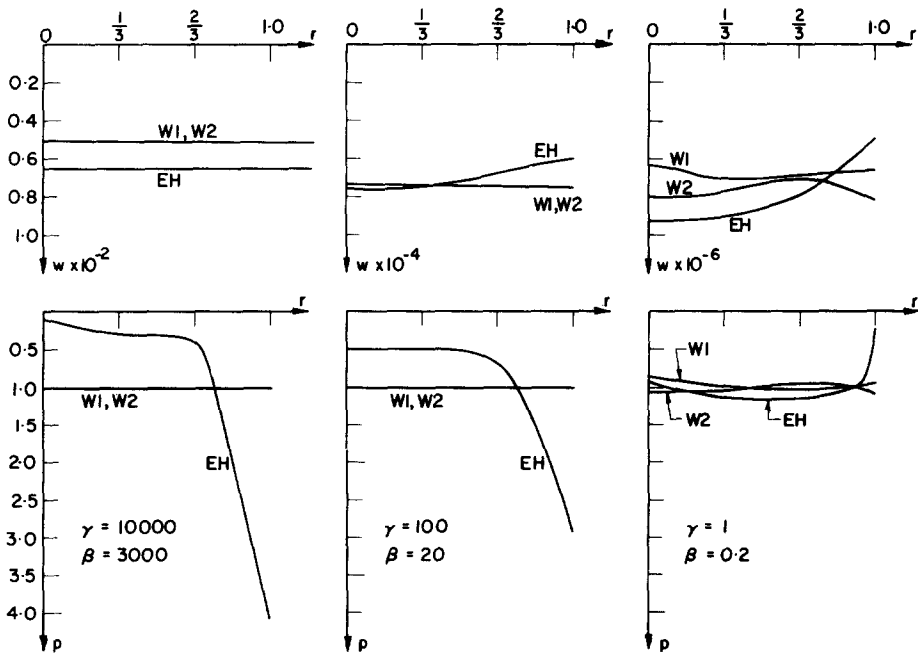


FIG. 4. The displacements and contact pressures for a circular plate under uniform loading.

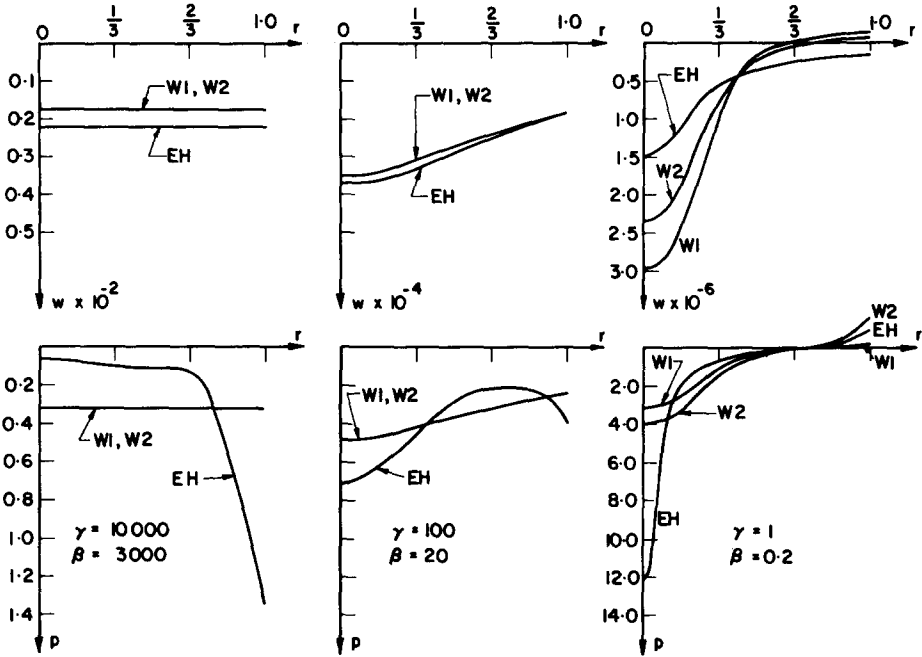


FIG. 5. The displacements and contact pressures for a circular plate under a point load.

The behaviour of the circular plate loaded by a point load in the plate centre is demonstrated for three elastic moduli ratios $\gamma = 10,000, 100, 1$ and $\beta = 3000, 20, 0.2$ in Fig. 5. If the plate is very rigid, e.g. $\gamma = 10,000$, the situation is very similar to that of the uniform load. If $\gamma = 100$, the contact pressure is just beginning to distribute itself from the plate edges to the centre under the load. In this case, deflections for all three foundation models are almost identical. By decreasing the coefficient $\gamma = E/E_0$, deflections as well as contact pressures become more and more different. For $\gamma = 10$ (not shown in Fig. 4) the contact pressure under the point load for the elastic half-space is about one-third that for the Winkler foundation which gives displacements of comparable magnitude ($\beta = 2$); for $\gamma = 1$ the ratio of central contact pressures has dropped to 1/4.

The central pressure for the modified Winkler model is a little nearer to that of the half-space, but there is still a significant difference between them.

There is another way to compare the results. Consider an arbitrary point (in this work the centroid of the circular plate is chosen) in which it is desired to show differences between various foundations. Using a log-log scale, plot the displacements at this point against the half-space ratio $\gamma = E/E_0$ and the Winkler ratio $\beta = E\pi/k(1 - \nu_0^2)$. Figure 6 shows that the curves corresponding to a uniform load are almost straight lines. If one now changes the scale for β one may shift the line corresponding to the Winkler model to make it close to the line for the elastic half-space. In this way, one can obtain an "equivalent" Winkler model for a specified elastic half-space. Of course, the equivalence applies only to the displacement at that particular point. However, if the displacements due to the two models are made equal at one point one may see the discrepancies between the models for pressures and for displacements at other points.

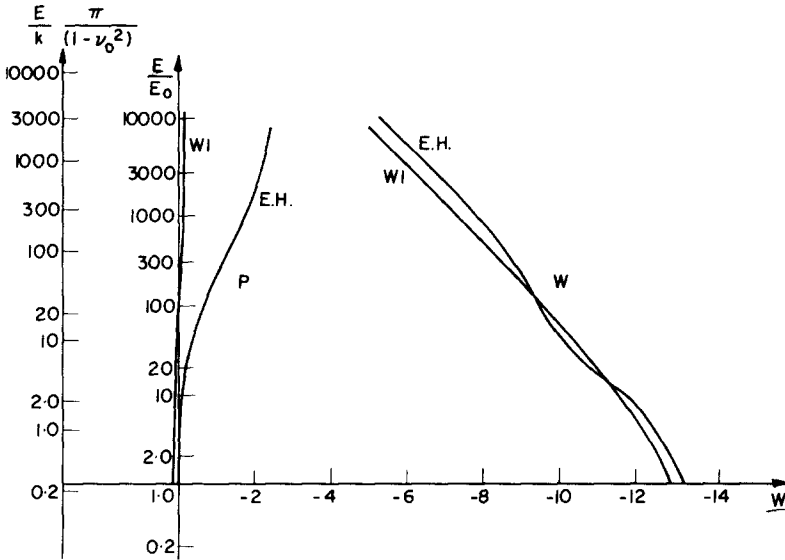


FIG. 6. The variation of displacement and pressure with elastic moduli ratios for the elastic half-space and Winkler models. Both variables are plotted in a log scale.

The relationship between the Winkler models and the elastic half-space for triangular and square plates was found to be very similar to that for the circular plate. Figures 7 and 8 show typical results for a triangular and square plate.

7. CONCLUSIONS

The plate finite element model was applied to the problem of a plate on an elastic half-space and two models of Winkler type. It was shown that for a rigid plate the main discrepancies between the contact pressure for the elastic half-space and Winkler models occur along the plate edges, no matter whether a uniform or a point load is applied. Secondly, for a point load on a weak plate, the greatest differences occur in contact pressures under the load. The deflections are now very different no matter which point is used to standardize the displacements for the half-space and Winkler model. We conclude on the basis of the more extensive computations reported in [8] that the pure Winkler model can be used as a representation of an elastic half-space only if the elastic moduli ratio $\gamma = E/E_0$ lies in a certain range. For the values ν , ν_0 , h taken in the calculations this range was roughly $10 \leq \gamma \leq 100$. The interval for γ can be taken somewhat larger for a circular plate, it decreases for a rectangular plate and is smallest for the triangular plate. The γ -interval for which Winkler's assumptions may be used is larger for a uniform load than for a point load. It was also found that the modified Winkler foundation described in this chapter usually gives better results than the pure Winkler model. The contact pressure using the modified Winkler model lies between results for pure Winkler model and the elastic half-space.

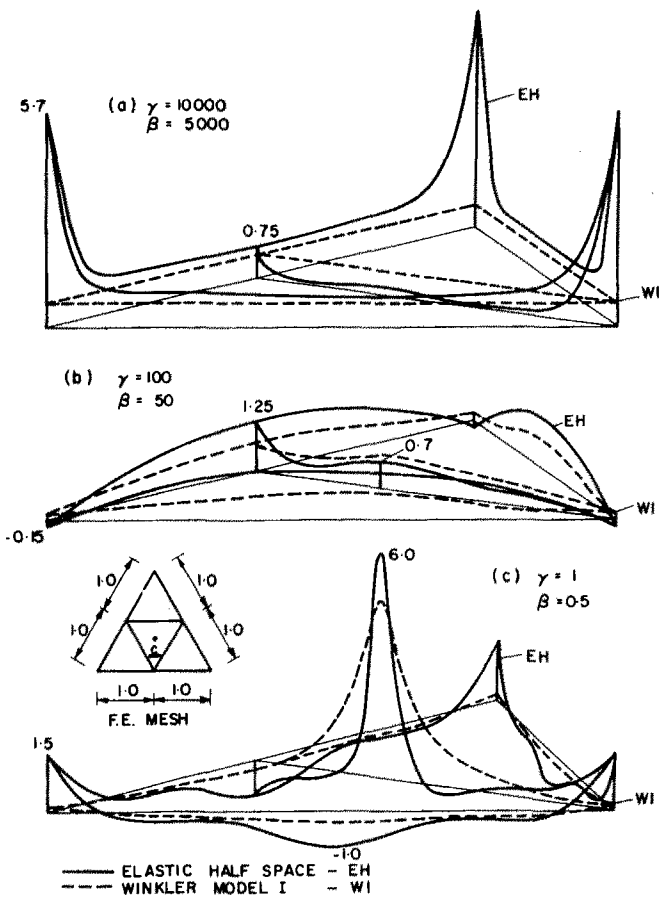


FIG. 7. The pressure distribution for a triangular plate under a point load at the centroid.

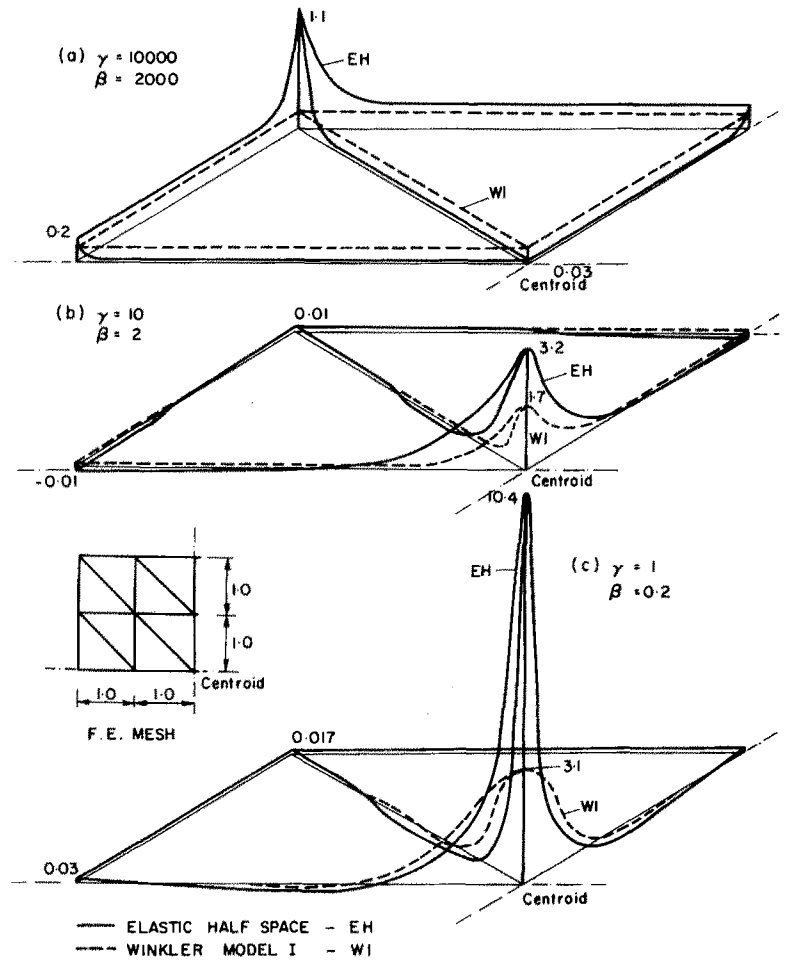


FIG. 8. The pressure distribution for a square plate under a point load at the centre.

REFERENCES

- [1] Y. K. CHEUNG and O. C. ZIENKIEWICZ, Plates and tanks on elastic foundation—an application of the finite element method. *Int. J. Solids Struct.* **1**, 451 (1965).
- [2] Y. K. CHEUNG and D. K. NAG, Plates and beams on elastic foundations—Linear and non-linear behaviour. *Geotechnique* **18**, 250 (1968).
- [3] R. CLOUGH and C. FELIPPA, A refined quadrilateral element for analysis of plates in bending. *Proc. 2nd Conf. on Matrix Methods in Struct. Mech., Wright Patterson AFB, Ohio* (October 1968).
- [4] O. J. SVEC and G. M. L. GLADWELL, An explicit Boussinesq solution for a polynomial distribution of pressure over a triangular region. *J. Elasticity* **1**, 167 (1971).
- [5] O. J. SVEC and G. M. MCNEICE, Finite element analysis of finite sized plates bonded to an elastic half space. To appear in *J. of Computer Methods in Applied Mechanics and Engineering*.
- [6] A. ŽENIŠEK, Interpolation polynomials on the triangle. *Num. Math.* **15**, 283 (1970).
- [7] G. R. COWPER, E. KOSKO, G. M. LINDBERG and M. D. OLSON, A high-precision triangular plate bending element. *N.R.C. Aeronautical Report LR-514*, Ottawa (1968).
- [8] O. J. SVEC, A finite element approach to the problem of a plate on an elastic half space. Ph.D. Thesis, Department of Civil Engineering, University of Waterloo, Ontario, Canada (1972).

(Received 1 November 1972; revised 19 June 1972)